

2

OFFICE OF NAVAL RESEARCH

Contract N00014-88-k-0482, Mod/Amend P00001

Technical Report No. 9

Electrochemistry Using Nanometer-Sized Electrodes

by

Reginald M. Penner, Michael J. Heben, Teresa L. Longin, and Nathan S. Lewis

Prepared for Publication in

Science.

California Institute of Technology
Department of Chemistry
Pasadena, California 91125

May 29, 1990

Reproduction in whole or in part is permitted for any purpose of the United States Government.

This document has been approved for public release and sale; its distribution is unlimited.

AD-A223 890

DTIC
ELECTE
JUN 05 1990
S D

REPORT DOCUMENTATION PAGE

1a. REPORT SECURITY CLASSIFICATION Unclassified			1b. RESTRICTIVE MARKINGS			
2a. SECURITY CLASSIFICATION AUTHORITY			3. DISTRIBUTION / AVAILABILITY OF REPORT Approved for Public Release and Sale. Distribution Unlimited			
2b. DECLASSIFICATION / DOWNGRADING SCHEDULE						
4. PERFORMING ORGANIZATION REPORT NUMBER(S) ONR Technical Report #9			5. MONITORING ORGANIZATION REPORT NUMBER(S)			
6a. NAME OF PERFORMING ORGANIZATION Nathan S. Lewis Caltech		6b. OFFICE SYMBOL (if applicable)	7a. NAME OF MONITORING ORGANIZATION			
6c. ADDRESS (City, State, and ZIP Code) Mail Code: 127-72 California Institute of Technology Pasadena, California 91125			7b. ADDRESS (City, State, and ZIP Code)			
8a. NAME OF FUNDING / SPONSORING ORGANIZATION Office of Naval Research		8b. OFFICE SYMBOL (if applicable)	9. PROCUREMENT INSTRUMENT IDENTIFICATION NUMBER N00014-88-k-0482, Mod/Amend: P00001			
8c. ADDRESS (City, State, and ZIP Code) Attention: Code 413 800 N. Quincy Street Arlington, VA 22217			10. SOURCE OF FUNDING NUMBERS			
			PROGRAM ELEMENT NO	PROJECT NO.	TASK NO	WORK UNIT ACCESSION NO
11. TITLE (Include Security Classification) Electrochemistry Using Nanometer-Sized Electrodes						
12. PERSONAL AUTHOR(S) Reginald M. Penner, Michael J. Heben, Teresa L. Longin, and Nathan S. Lewis						
13a. TYPE OF REPORT Technical		13b. TIME COVERED FROM June 89 TO May 90	14. DATE OF REPORT (Year, Month, Day) 1990, May 29		15. PAGE COUNT 15	
16. SUPPLEMENTARY NOTATION						
17. COSATI CODES			18. SUBJECT TERMS (Continue on reverse if necessary and identify by block number) ultramicroelectrode, nanode, heterogeneous electron transfer rate constant, steady-state, kinetics			
FIELD	GROUP	SUB-GROUP				
19. ABSTRACT (Continue on reverse if necessary and identify by block number) Electrodes with dimensions as small as 10 Å have been fabricated and used for electrochemical studies. Remarkably large current densities are generated by these ultra small electrodes, as predicted by conventional radial diffusion theory. These large current densities have enabled the measurement of electron transfer rate constants, k_{het} , which are two orders of magnitude faster than k_{het} values accessible using any other electrochemical method.						
20. DISTRIBUTION / AVAILABILITY OF ABSTRACT <input checked="" type="checkbox"/> UNCLASSIFIED/UNLIMITED <input type="checkbox"/> SAME AS RPT <input type="checkbox"/> DTIC USERS			21. ABSTRACT SECURITY CLASSIFICATION Unclassified			
22a. NAME OF RESPONSIBLE INDIVIDUAL			22b. TELEPHONE (Include Area Code)		22c. OFFICE SYMBOL	

Electrochemistry Using Nanometer-Sized Electrodes

Reginald M. Penner, Michael J. Heben, Teresa L. Longin, and Nathan S. Lewis*

Division of Chemistry and Chemical Engineering

California Institute of Technology

Pasadena, CA 91125

ABSTRACT

Electrodes with dimensions as small as 10 Å have been fabricated and used for electrochemical studies. Remarkably large current densities are generated by these ultra small electrodes, as predicted by conventional radial diffusion theory. These large current densities have enabled the measurement of electron transfer rate constants, k_{het} , which are two orders of magnitude faster than k_{het} values accessible using any other electrochemical method.

Accession For	
NTIS CRA&I	<input checked="" type="checkbox"/>
DTIC TAB	<input type="checkbox"/>
Unannounced	<input type="checkbox"/>
Justification	
By _____	
Distribution /	
Availability Codes	
Dist	Avail and/or Special
A-1	



* Author to whom correspondence should be addressed.

Ultra-small electrodes are being increasingly used in areas as diverse as scanning tunneling microscopy (1), electrophysiology (2), chemical kinetics (3), and nanolithography (4). The temporal and spatial advantages of small electrodes have allowed electrochemists to measure the rates of fast chemical reactions (3,5,6), to perform *in-vivo* voltammetric measurements inside living brain tissue (7) and inside single cells (8), to observe changes in the conductivity of single ion channels (9), to efficiently detect analytes eluted from a capillary zone electrophoresis column (10), and to perform small scale etching and lithography (4). In all of these applications, the performance of the electrode with respect to speed and spatial resolution scales inversely with the electrode radius. The smallest ultramicroelectrodes with well-defined voltammetry reported to date have an exposed radius of $0.1 \mu\text{m}$ (11), with more typical sizes in the range $1.0\text{-}10.0 \mu\text{m}$. In this report, we describe a method that has allowed the routine fabrication of electrodes with radii as small as 10 \AA . We also describe the use of these nanometer-scale electrodes (nanodes) to determine electron transfer rate constants which are two orders of magnitude faster than those accessible with any other currently available electrochemical method.

The nanodes were fabricated in a two step procedure. 0.50 mm diameter Pt or Pt-Ir (70:30) wire was first electrochemically sharpened using an AC etching procedure, as described previously (12,13). Etched wires were then translated at 0.10 mm/s through a molten glass bead that was held in a resistively heated, circular Pt filament (i.d. $\approx 2 \text{ mm}$). The size of the aperture in the resultant glass coating was related to the translation velocity and to the temperature of the molten glass: at a constant wire translation velocity, the effective aperture radius, r , increased with increasing insulator melt temperature. Temperatures in the range $1250\text{-}1370 \text{ }^\circ\text{C}$ were used to prepare electrodes with radii of $10 \text{ \AA} - 20 \mu\text{m}$. This two step etching and coating process closely resembles standard procedures used to prepare $1\text{-}50 \mu\text{m}$ diameter glass-coated Pt electrodes for neurophysiology applications (14), except that the refinements in procedure described above yielded electrodes with much smaller exposed metal areas. Control of the relationship between glass melt temperature and r readily enabled the fabrication of small apertures in high yield: $\approx 50\%$ of the electrodes fabricated possessed radii of $< 0.10 \mu\text{m}$ (*vide supra*), and approximately 10% (out of over 200 electrodes fabricated in our laboratory) exhibited radii in the range $10\text{-}100 \text{ \AA}$.

Figure 1 displays optical and scanning electron microscope (SEM) images of a typical nanode produced by this procedure. The apex of this electrode had an ultimate hemispherical radius of $\approx 0.2 \mu\text{m}$, and appeared to be completely covered with glass even at the highest magnifications available with the SEM (50,000x). However, this specimen was not totally insulating when used as an electrode, but exhibited conventional steady-state microelectrode behavior. The voltammetry of representative nanodes in several electrolytes containing redox active ions is shown in Figure 2. The mass transport controlled limiting current, i_l , measured from the plateau region of the sigmoidal steady state voltammogram, can be related to the effective radius of exposed metal using equation [1] (15):

$$[1] \quad i_l = 2\pi nFD C^* r$$

where $F = 96487 \text{ C/eq.}$, D is the diffusion coefficient of the reactant (cm^2/s), C^* is the bulk concentration of the reactant (moles cm^{-3}), and r is the electrochemical radius (cm). Equation [1] was used to calculate electrochemical radii of $1.9 \mu\text{m}$ and $17.4 \mu\text{m}$ for the electrodes in Fig. 2a, and of 16 \AA and $3.0 \mu\text{m}$ for the electrodes in Fig. 2b. To validate this calculation, several (>10) nanodes were measured in one electrolyte and were then transferred to a solution containing a different redox couple; agreement between the calculated r values in these independent measurements was typically within 20%. A tacit assumption implied in the use of equation 1 is that the electrode has a hemispherical geometry. The assumption of other exposed metal geometries (e.g. disk, cone) would yield apparent electrode radii which are larger by 20-30% than the values obtained from Equation 1 (the factor 2π would be replaced by 4.0 for a disk (16) and by $\approx 2\pi$ for a cone (13)), but this does not affect the primary conclusion that extremely small electrodes have been prepared by the etching/coating method.

Although the absolute magnitude of the current for these nanodes is small, the current densities are extremely large. The 70 A cm^{-2} current density obtained in Figure 2c exceeds, by two orders of magnitude, the current densities accessible in this electrolyte with a rotating disk electrode or with AC potential modulation methods (17), and corresponds to a mass transport velocity, $m_0 (= D/r)$, of 100 cm/s . The large m_0 values generated by nanodes extends the range of maximum measurable electron transfer rate constants (k_{het}), because the rate of electron transfer is less likely to be limited by mass

transport of the reactant to the electrode surface. Smaller electrodes are advantageous because the current density is inversely related to the electrode radius, implying that the maximum measurable value of k_{het} increases linearly with $1/r$. Moreover, since the extraction of kinetic information from steady-state voltammograms does not require severe correction for resistance and capacitance effects, nor the construction of extremely high speed (>MHz) potentiostats, nanode based kinetic measurements are both straight forward and reliable (18). Nanodes with radii of 10 Å, described in this Report, are capable of measuring k_{het} values that are within a factor of 6 of the values attainable using a hypothetical single platinum atom ($r = 1.53 \text{ \AA}$) as an electrode.

Figure 2a-c displays the complete steady state voltammetry for a collection of different nanodes in contact with a variety of electrolytes. As expected, when the electrode radius was sufficiently large, mass transport limited (i.e. Nernstian) electrode behavior was observed, and the peak shape and position on the potential axis was independent of further increases in electrode radius (dashed curves, Figure 2a-c). No quantitative kinetic information can be obtained from such voltammetric data.

In contrast, when the electrode radius becomes comparable to the value of D/k_{het} (19), mass transport is sufficiently rapid that the wave shape is no longer independent of electrode radius, and k_{het} can be determined from an analysis of the voltammogram shape and its position on the potential axis (19,20). The exact equations for calculating kinetic voltammograms at microelectrodes have been derived by Zoski and Oldham (21), and we have used this theory to extract values of k_{het} and α from the steady-state nanode data. The magnitude of the potential shift at the formal potential, $E^{0'}$, was used to evaluate k_{het} , while the slope of $\ln(k_{het})$ vs. $E^{0'}$ in the potential interval $\pm 10 \text{ mV}$ of $E^{0'}$ was used to evaluate the value of the transfer coefficient, α (21). Best-fit voltammograms obtained using this procedure are displayed as solid lines through the experimental data in Figures 2a-c. The fit of the calculated I-V curve to the experimental data was not very sensitive to α which ranged from 0.5 - 0.7. Values of the heterogeneous rate constants obtained for the three redox couples depicted in Figure 2, and for the other redox couples investigated in this work, are summarized in Table I.

Kinetic parameters for relatively slow electron transfer reactions ($k_{het} < 0.5 \text{ cm/s}$) have been measured previously using conventional electrochemical methods. Our measurements of two k_{het} values reported to be in the range $k_{het} = 10^{-3}$ - 10^{-1} cm/s were in good agreement with those of previous

workers (Table I). These measurements employed electrodes with radii at the large end of the range used in our work: electrodes with radii of 1.0 - 2.0 μm were sufficient to measure k_{het} for $\text{Ru}(\text{NH}_3)_6^{3+/2+}$ in 50 mM $\text{KPF}_6(\text{aq})$ and k_{het} for $\text{Fe}^{3+/2+}$ in 0.1 M $\text{H}_2\text{SO}_4(\text{aq})$. Weaver and coworkers (22) have observed dramatic increases in k_{het} for cobalt amine complexes in aqueous electrolytes containing Cl^- , however the magnitude of this effect for $\text{Ru}(\text{NH}_3)_6^{3+/2+}$ could not be quantified because k_{het} in 0.5 M $\text{KCl}(\text{aq})$ is too large to be measured using conventional techniques (23). In contrast to the kinetic data of Figure 2a (obtained with a 1.9 μm radius electrode), substantially smaller electrodes were required to observe kinetic voltammograms in $\text{Ru}(\text{NH}_3)_6^{3+/2+}$ solutions containing 0.5 M KCl . Kinetic voltammograms were obtained using 10-20 \AA radius nanodes, and these data yielded a value for k_{het} of (79 ± 44) cm/s (Figure 2, Table I). A lower limit for the heterogeneous rate constant for ferrocene $^{+/0}$ ($\text{Fc}^{+/0}$) of > 10 cm/s has been estimated by Bond et al. (24) using steady-state voltammetry at microelectrodes with $r = 0.3 \mu\text{m}$. Our measurements at 15-20 \AA radius nanodes yielded a value for k_{het} of (220 ± 120) cm/s in CH_3CN , 0.10 M $[(n\text{-C}_4\text{H}_9)_4\text{N}][\text{ClO}_4]$ electrolyte. In contrast to $\text{Ru}(\text{NH}_3)_6^{3+/2+}$ and $\text{Fc}^{0/+}$, both methyl viologen $^{2+/+}$ ($\text{MV}^{2+/+}$) and 1,1'-dicarbomethoxycobaltocene $^{+/0}$ ($\text{Cp}^\#_2\text{Co}^{+/0}$) exhibited reversible voltammetric behavior even at nanodes with radii $\approx 20 \text{\AA}$, indicating that $k_{het} > (170 \pm 90)$ cm/s for $\text{MV}^{2+/+}$ and $k_{het} > (130 \pm 70)$ cm/s for $\text{Cp}^\#_2\text{Co}^{+/0}$. These data are useful because the Nernstian response observed at the smallest electrodes indicates that the kinetic voltammetry obtained for other systems at 10-50 \AA nanodes is not an artifact resulting from unusual voltammetric responses at nanometer-sized electrodes. No evidence for a dependence of k_{het} on the electrode dimension was observed for the electrolyte concentrations and nanode radii used in this work (25).

These k_{het} values are in good agreement with expectations based on electron transfer theories. Marcus (26) has derived a relationship between homogeneous self-exchange electron transfer rate constants (k_{ex}) and heterogeneous rate constants:

$$[2] \quad k_{het} = Z_{het}(k_{ex}/Z_{bi})^{1/2}$$

where Z_{bi} is the bimolecular collision frequency, $10^{11} \text{ M}^{-1}\text{s}^{-1}$, and Z_{het} is the unimolecular collision frequency into a surface, 10^4 cm/s . The validity of this relationship was questioned by earlier heterogeneous kinetic measurements (27) that were later disputed as being limited by the time response of the technique. The self-exchange rates (k_{ex}) for $\text{Fe}^{3+/2+}$ ($\approx 3 \text{ M}^{-1}\text{s}^{-1}$ (28,29)) and $\text{Ru}(\text{NH}_3)_6^{3+/2+}$ ($\approx 4 \times 10^3 \text{ M}^{-1}\text{s}^{-1}$ (30,31)) can be used in equation [2] to predict k_{het} values of 0.05 cm/s and 2 cm/s respectively, which are in reasonable agreement with the experimental values obtained in this work and measured previously (Table I). Similarly, k_{ex} for $\text{Fc}^{+/0}$ ($8.5 \times 10^6 \text{ M}^{-1}\text{s}^{-1}$ (32)) corresponds to $k_{het} = 90 \text{ cm/s}$ and k_{ex} for 1,1'-dicarbomethoxycobaltocene $^{+/0}$ ($1.9 \times 10^8 \text{ M}^{-1}\text{s}^{-1}$, (33)) yields a value for k_{het} of $> 400 \text{ cm/s}$, which is consistent with the observed voltammetric behavior. The indirect estimates of k_{ex} for methyl viologen $^{2+/+}$ ($k_{ex} = 8.0 \times 10^6 \text{ M}^{-1}\text{s}^{-1}$ (34)) predict a k_{het} of 89 cm/s, which is somewhat smaller than the lower limit of $(170 \pm 90) \text{ cm/s}$ which we report here. Although the overall consistency of equation [2] is indicated by these new k_{het} measurements, more kinetic data is required to quantitatively test its validity under a variety of conditions. We note, however, that self-exchange kinetic measurements for most outer-sphere redox ions predict k_{het} values which are too large to measure using conventional methods, but which can now be determined using nanodes and the steady-state voltammetric method described above.

In conclusion, we have demonstrated that nanometer-sized electrodes can be reproducibly fabricated, and subsequently characterized by electrochemical methods. These nanodes can be used to obtain heretofore unavailable kinetic information on a range of redox couples. Additionally, they should find application in a variety of areas, including neurophysiology, lithography, chemical analysis, and scanning tunneling microscopy, and will help advance the methodology to construct and modify physical and chemical structures on a molecular scale.

Acknowledgments: We acknowledge the Office of Naval Research for support of this work, and Professors F.C. Anson of Caltech and M.J. Weaver of Purdue University for helpful discussions. This is contribution #8153 from the Division of Chemistry and Chemical Engineering at Caltech.

References and Notes

1. R. Sonnenfeld, B.C. Schardt, *Appl. Phys. Lett.* **49**, 1172 (1986); P. Lustenberger, H. Rohrer, R. Christoph, H. Siegenthaler, *J. Electroanal. Chem.* **243**, 225 (1988); M.J. Heben, R.M. Penner, N.S. Lewis, M.M. Dovek, C.F. Quate, *Appl. Phys. Lett.* **54**, 1421 (1989).
2. A.M. Mamoan, W.T. Schlapfer, B.H. Fahwiler, C.A. Tobias, *Adv. Biol. Med. Phys.* **16**, 1 (1977); B. Sackmann, E. Neher, *Ann. Rev. Physiol.* **46**, 455 (1984).
3. A. Fitch, D.H. Evans, *J. Electroanal. Chem.* **202**, 83 (1986); W.J. Bower, E.E. Engelman, D.H. Evans, *J. Electroanal. Chem.* **262**, (1989) 67; C.P. Andrieux, P. Hapiot, J.M. Saveant, *J. Phys. Chem.* **92**, 5987 (1988); C.P. Andrieux, P. Hapiot, J.M. Saveant, *J. Phys. Chem.* **92**, 5992 (1988);
4. C.W. Lin, F.R. Fan, A.J. Bard, *J. Electrochem. Soc.* **134**, 1038 (1987); D.H. Craston, S.W. Lin, A.J. Bard, *J. Electrochem. Soc.* **135**, 785 (1988); J. Schneir *et al.*, *Proc. SPIE* **897**, 16 (1988).
5. D.O. Wipf, E.W. Kristensen, M.R. Deakin, R.M. Wightman, *Anal. Chem.* **60**, 306 (1988).
6. D.O. Wipf, R.M. Wightman, *Anal. Chem.* **60**, 2460 (1988); C.P. Andrieux, D. Garreau, P. Hapiot, J. Pinson, J.M. Saveant, *J. Electroanal. Chem.* **243**, 321 (1988)
7. P.T. Kissinger, J.B. Hart, R.N. Adams, *Brain Res.* **55**, 209 (1973); J.C. Conti, E. Strope, R.N. Adams, C.A. Marsden, *Life Sci.* **23**, 2705 (1978); A.G. Ewing, R.M. Wightman, M.A. Dayton, *Brain Res.* **249**, 361 (1982).
8. K. Tanaka, N. Kashiwagi, *Bioelectrochem. Bioenerg.* **17**, 519 (1987); K. Tanaka, N. Kashiwagi, *Bioelectrochem. Bioenerg.* **21**, 95 (1989).
9. E. Neher, B. Sackman, *Nature* **260**, 779 (1976); E. Neher, B. Sackman, J.H. Steinbach, *Plügers Arch. ges. Physiol.* **375**, 219 (1978); F. Conti, E. Neher, *Nature* **285**, 140 (1980).
10. R.A. Wallingford, A.G. Ewing, *Anal. Chem.* **60**, 1972 (1988); R.A. Wallingford, A.G. Ewing, *Anal. Chem.* **60**, 258 (1988).
11. A.A. Gewirth, D.H. Craston, A.J. Bard, *J. Electroanal. Chem.* **261**, 477 (1989); F.R. Fan, A.J. Bard, *J. Electrochem. Soc.* **136**, 3216 (1989); M. Fleischmann, S. Pons,

- D.R. Rolison, P.P. Schmidt, *Ultramicroelectrodes* (Datatech Systems, Inc., Morgantown, NC, 1987) Chapter 3.
12. M.J. Heben, M.M. Dovek, N.S. Lewis, R.M. Penner, C.F. Quate, *J. Microsc.* **152**, 651 (1988); M.J. Heben, Ph.D. Thesis, California Institute of Technology, March 1990.
 13. R.M. Penner, M.J. Heben, N.S. Lewis, *Anal. Chem.* **61**, 1630 (1989).
 14. M.L. Wolbarsht, E.F. MacNichol Jr., H.G. Wagner, *Science* **132**, 1309 (1960); C. Guld, *Med. Electron. Biol. Eng.* **2**, 317 (1964).
 15. W.H. Reinmuth, *J. Am. Chem. Soc.* **79**, 6358 (1957).
 16. M.A. Dayton, J.C. Brown, K.J. Stutts, R. M. Wightman, *Anal. Chem.* **52**, 946 (1980).
 17. A.J. Bard and L.R. Faulkner *Electrochemical Methods* (J. Wiley & Sons, Inc., New York, 1980) Chaps 5,6,8,9.
 18. Experimental problems associated with the determination of k_{het} using cyclic voltammetry, for example, are discussed in the following references: D.F. Milner, M.J. Weaver, *Analytica Chimica Acta* **198**, 245 (1987); J.O. Howell, W.G. Kuhr, R.E. Ensman, R.M. Wightman, *J. Electroanal. Chem.* **209**, 77 (1986); A.M. Bond *et al.*, *Anal. Chem.* **60**, 1878 (1988).
 19. A. Russell *et al.*, *Anal. Chem.* **58**, 2961 (1986); K.B. Oldham, C.G. Zoski, A.M. Bond, D.A. Sweigart, *J. Electroanal. Chem.* **248**, 467 (1988).
 20. Z. Galus, J. Golas, J. Osteryoung, *J. Phys. Chem.* **92**, 1103 (1988).
 21. K.B. Oldham, C.G. Zoski, *J. Electroanal. Chem.* **256**, 11 (1988) 11.
 22. M.J. Weaver, T.L. Satterberg, *J. Phys. Chem.* **81**, 1772 (1977); M.J. Weaver, *J. Electroanal. Chem.* **93**, 231 (1978); T.L. Satterberg, M.J. Weaver, *J. Phys. Chem.* **82**, 1784 (1978); S.W. Barr, K.L. Guyer, M.J. Weaver, *J. Electroanal. Chem.* **111**, 41 (1980).
 23. T. Gennett, M.J. Weaver, *Anal. Chem.* **56**, 1444 (1984).
 24. A.M. Bond *et al.*, *Anal. Chem.* **60**, 1878 (1988).
 25. R.B. Morris, D.J. Franta, H.S. White, *J. Phys. Chem.* **91**, 3559 (1987); J. Duke, E.R. Scott, H.S. White, *J. Electroanal. Chem.* **264**, 281 (1989).
 26. R.A. Marcus, *J. Phys. Chem.* **67**, 853 (1963); R.A. Marcus, *Ann. Rev. Phys. Chem.* **15**, 155 (1964).

27. T. Saji, T. Yamada, S. Aoyagui, *J. Electroanal. Chem.* **61**, 147 (1975); T. Saji, *J. Electroanal. Chem.* **86**, 219 (1978).
28. J. Silverman, R.W. Dodson, *J. Phys. Chem.* **56**, 846 (1952).
29. B.S. Brunshwig, C. Creutz, D.H. Macartney, T.K. Sham, N. Sutin, *Faraday Disc. Chem. Soc.* **74**, 113 (1982);
30. J.T. Hupp, M.J. Weaver, *J. Phys. Chem.* **93**, 4703 (1989).
31. T.J. Meyer, H. Taube, *Inorg. Chem.* **7**, 2369 (1968).
32. R.M. Neilson, G.E. McMannis, L.K. Safford, M.J. Weaver, *J. Phys. Chem.* **93**, 2152 (1989).
33. R.M. Neilson, G.E. McMannis, M.J. Weaver, *J. Phys. Chem.* **93**, 4703 (1989).
34. C.R. Bock *et al.*, *Chem. Phys. Lett.* **61**, 522 (1979).
35. Z. Samec, J. Weber, *J. Electroanal. Chem.* **77**, 163 (1977).
36. D.H. Angell, T. Dickinson, *J. Electroanal. Chem.* **35** 55 (1972).
37. M.I. Montenegro, D. Pletcher, *J. Electroanal. Chem.* **200**, 371 (1986).

Table I. Measured k_{het} data, comparison with literature values of k_{het} , and comparison with k_{het} values calculated from equation 2 using literature values of k_{ex} .

Redox Couple	Electrolyte	electrode radius ^a	ΔE^b (mV)	k_{het}^c (cm s ⁻¹)	k_{het} (lit.) ^d (cm s ⁻¹)	Reference	k_{ex} (lit.) ^e (M ⁻¹ s ⁻¹)	k_{het} (calc.) ^f (cm s ⁻¹)	Reference
Fe ^{3+/2+}	0.1 M H ₂ SO ₄ , aqueous	18 μm	10	0.018					
		8.1 μm	14	0.022					
		2.0 μm	30	0.031					
		1.3 μm	44	<u>0.029</u>					
				0.018 ± 0.007	0.018 - 0.0032	(19,34,35)	1.1, 4.2	0.033, 0.065	(28,27)
Ru(NH ₃) ₆ ^{3+/2+}	50 mM KPF ₆ , aqueous	4.6 μm	6	0.10					
		3.7 μm	6	0.12					
		1.6 μm	4	0.38					
		1.3 μm	10	<u>0.17</u>					
				0.26 ± 0.13	0.35, 0.45	(22,5)	3200, 4300	1.8, 2.5	(30,29)
Ru(NH ₃) ₆ ^{3+/2+}	0.5 M KCl, aqueous	1.1 μm	0	> 0.13					
		269 Å	0	> 9.3					
		203 Å	0	> 11					
		11 Å	37	<u>47</u>					
				79 ± 44	-		-	-	
Fc ^{+/0}	0.3 M Bu ₄ NClO ₄ , acetonitrile	2.6 μm	0	> 0.22					
		0.57 μm	0	> 1.1					
		18 Å	28	120					
		16 Å	17	<u>220</u>					
				220 ± 120	0.7 - 3.1	(27,37,5)	8.5 × 10 ⁶	90	(32)
MV ^{2+/+}	0.1 M Bu ₄ NClO ₄ , acetonitrile	0.21 μm	0	> 1.8					
		0.11 μm	0	> 3.6					
		67 Å	0	> 58					
		22 Å	0	<u>> 170</u>					
				> 170 ± 90	-		8.0 × 10 ⁶	89	(34)
(CpCOOCH ₃) ₂ Co ^{+/0}	0.1 M Bu ₄ NClO ₄ , acetonitrile	4.7 μm	0	> 0.066					
		280 Å	0	> 10					
		37 Å	0	> 77					
		23 Å	0	<u>> 130</u>					
				> 130 ± 70	-		1.9 × 10 ⁶	430	(33)

^aCalculated from the measured limiting current, i_L , using Equation [1].

^bShift in potential of the steady-state voltammogram relative to E^0 at a reversible (Nernstian) voltammogram. Tabulated are the observed shifts for four electrodes of various sizes.

^cHeterogeneous electron transfer rate constants (uncorrected for double layer effects) as measured using steady-state voltammetry. Tabulated are four representative k_{het} values corresponding to the potential shifts listed in column 4. The average k_{het} value and 1σ standard deviations listed are statistics for larger data sets of up to 10 measurements. For electrodes that exhibited no potential shift, a lower limit of k_{het} is listed. In such cases, the lower limit was estimated as the value of k_{het} required to induce a 10 mV shift at E^0 .

^dValues of k_{het} reported in previous published work.

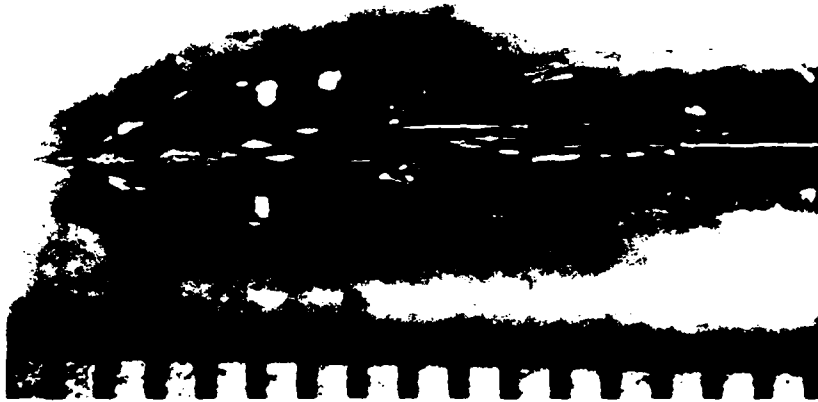
^eElectron self-exchange rate constants reported in previous published work.

^fValues for k_{het} calculated from k_{ex} using the Marcus cross-relation, equation [2].

Figure 1. Optical (A) and scanning electron (B) micrographs of a typical nanode. The vertical bars in (A) are at intervals of 0.50 mm.

Figure 2. Voltammetric behavior (5 mV/s) of several nanodes in various electrolytes. Each voltammogram was normalized to the value of i_l after subtraction of a sloping baseline. Concentrations of redox species were as follows: (A) open circles: 6.67 mM; closed circles: 6.51 mM. (B) open circles: 4.30 mM; closed circles: 2.97 mM. (C) open circles: 3.54 mM; closed circles: 3.45 mM. In (B) and (C), the fit to the open circle data was unchanged for all electrodes with radii $> 50 \text{ \AA}$, and was in excellent agreement with the Nernstian behavior (dashed line) generated by using the value of $E^{0'}$ obtained from voltammetric measurements at the largest nanode radii. In (A), the Nernstian voltammogram (dashed line) was determined by measurement of $E^{0'}$ using cyclic voltammetry, because k_{het} for $\text{Fe}^{3+/2+}$ is so small that kinetic voltammograms were obtained even at the largest microelectrodes used in this work. In (A)-(C), the deviations observed from ideal Nernstian behavior allow determination of k_{het} .

A.



B.



| <----> |
1000 A

